Hindawi
Wireless Communications and Mobile Computing
Volume 2021, Article ID 9057264, 11 pages
https://doi.org/10.1155/2021/9057264

Research Article

Image Analysis Technology in the Detection of Particle Size Distribution and the Activity Effect of Low-Silicon Copper Tailings

Yuxiang Zhao,[1] Xinzhong Liu,[1] Biwen Liu,[1] Qian Zhang,[2] Dongdong Huan,[1] and Chenhui Qiu[1]

[1]*School of Ecological Environment and Urban Construction, Fujian University of Technology, Fuzhou 350000, China*
[2]*College of Environment & Safety Engineering, Fuzhou University, Fuzhou 350000, China*

Correspondence should be addressed to Xinzhong Liu; liuxinzh01@163.com

Received 8 October 2021; Accepted 18 November 2021; Published 9 December 2021

Academic Editor: Haibin Lv

To speed up the comprehensive utilization and treatment of copper tailings, the digital image processing technology is proposed in this study to detect the low-silicon copper tailings (LSCT) using a scanning electron microscope (SEM), and the particle size distribution (PSD) and the activity of LSCT are analysed under the action of mechanical force. Firstly, the current status and application of copper tailings are introduced, and the influence of the particle size of LSCT on its practical application performance is explained. Secondly, the LSCT SEM image target recognition model is designed based on the convolutional neural network (CNN), and the model parameters and the reference CNN are selected. Finally, the experimental process is designed, a SEM image data set of LSCT is prepared, the model is trained through the training set, and the image recognition test is performed on the produced data set. The experimental results show that when the number of iterations of the CNN is 10, the accuracy of model recognition can be guaranteed. After the action of mechanical force, the PSD of LSCT is mainly concentrated at 1 μm~100 μm; that around 1.4 μm~10 μm is the largest, and the PSD of LSCT around 1.4 μm increases with the increase of action time of mechanical force, but the PSD of the LSCT begins to increase when the grinding time exceeds 150 minutes, and the activity of LSCT reaches the maximum (75.545%) at 150 minutes. The average accuracy of SEM image detection of the model is 86.97%, and the model based on DenseNet shows better recognition accuracy than other models. This study provides a reference for analysing the PSD of LSCT.

1. Introduction

With the development of social productivity and the improvement of the level of science and technology, the types and quantities of mineral resources used by mankind are increasing, and the scope of utilization is also wider and wider. Iron, copper, manganese, nickel, chromium, and other mineral resources that play important roles in the development of the national economy are large in storage and mining, but the grade of the ore is generally low, and it can be used as smelting raw materials after beneficiation and processing [1]. Therefore, a large number of tailings are produced. If these tailings are not processed in time, they will not only occupy the land resources of Baohui but also cause serious pollution to the surrounding ecological environment. China produces hundreds of millions of tons of copper tailing waste every year in the process of beneficiation, and the reuse rate of copper tailings is not high due to the limitations of production conditions and technical capabilities [2]. How to more efficiently recycle resources of LSC tailings is an important problem that plagues the industry. The economic burden and pollution caused by the stacking of low-silicon copper (LSC) tailings also affect the development of local enterprises [3]. Therefore, the treatment of tailings has been urgently needed. How to turn them into treasures and form huge economic and social benefits is a key problem that needs to be solved at present [4]. In recent years, foreign countries have attached great importance to the comprehensive

utilization technology of tailings and achieved obvious economic and social benefits. China has also made good progress in the comprehensive recovery and utilization of tailing resources.

At present, experts and scholars all over the world have conducted extensive research on the comprehensive utilization of copper tailings. Li et al. studied a gradual extraction process to extract valuable metals such as copper, iron, lead, and zinc from copper tailings. Firstly, the flotation process is used to enrich copper; the flotation tailings are combined with limestone pelletizing; then, the green pellets are reduced, and then, the magnetic separation process is processed; 91.34% iron and 83.41% copper are recovered, respectively; finally, the nonmagnetic tailings are mixed with clinker and standard sand to make Portland concrete for construction [5]. Li et al. studied environmentally friendly building materials made from copper tailings and iron tailings and used X-ray Diffraction (XRD), Fourier Transform Infrared Spectroscopy (FTIR), and SEM techniques to characterize the microstructure and activity of the designed building materials; the experimental results showed that when the mass ratio is 1 : 4, the mixed tailing material shows better mechanical properties; three-dimensional crystals are formed between the mixed materials for close connection, which improves the mechanical properties of the material [6]. Lv et al. studied the use of tailings to replace ordinary aggregates to construct dam concrete projects and analysed the effects of tailing aggregates and natural aggregates on the performance of dam concrete; the experimental results showed that compared with natural aggregate concrete, tailing aggregate concrete has higher specific gravity and water consumption; the mechanical properties, ultimate tensile strain, compressive modulus of elasticity, and frost resistance of tailing aggregate concrete are similar to those of natural aggregate concrete, but the consumption of cementitious materials is small, and it also has good thermal properties [7]. Xu et al. studied the recycling of tailing resources from the three aspects of metal recycling, agricultural fertilizers, and building materials; these strategies are used to reduce environmental pollution caused by tailing stacking, so as to achieve sustainable mining [8]. Fisonga et al. studied the use of copper tailings to prepare highway concrete traffic guardrails and studied the gel properties of copper tailing concrete; the SEM results showed that the percentage of copper tailing concrete is reduced from 28.77% to 19.73%, which affected the rapid formation of calcium silicate hydration and the hydration concealed phase of etlingite [9]. Chen et al. studied the use of image processing technology to evaluate the geological features of shale samples in scanning electron microscopy images and to identify clay aggregates mixed with matrix mineral particles and organic matter; its ability to distinguish geological features is improved by designing and optimizing models; and this study could provide a reference for quantitative analysis of specific geological features and characteristics [10].

Based on the current research, the main factor affecting the performance of copper tailing concrete is the tailing performance. Therefore, in the study, LSC tailings are used as the research objects, and the PSD of LSC tailings under the action of mechanical force and the activity properties of the LSC tailings are analysed. In addition, it is proposed to use a convolutional neural network (CNN) to analyse the scanning electron microscope images of LSC tailings to obtain effective analysis data to improve the efficiency and accuracy of LSC tailing particle size analysis. The characterization experiment and mineral powder activity index experiment are performed to analyse the PSD and performance of LSC tailings under the action of mechanical force.

2. Research on PSD Recognition of LSC Tailings Based on Image Technology

2.1. Current Status and Treatment Methods of Copper Tailings. The copper resources in China are relatively small, but a large amount of copper tailing waste is generated every year during the mining and beneficiation process, which has a serious impact on the ecological environment. Copper tailings are the main component of industrial wastes in the copper mining industry and are the remaining wastes after obtaining useful minerals after beneficiation [11]. The copper resources are widely distributed in China, and the provinces with a large amount of copper tailings mainly include Jiangxi Province, Yunnan Province, Hubei Province, Gansu Province, and Anhui Province. Although the output of copper tailings in China is huge, domestic enterprises do not have the corresponding comprehensive recycling technology. The comprehensive utilization rate of copper tailings by foreign-related companies is 80%, while only 10% of Chinese companies have recycled copper tailings, and the recovery rate is only 8%. Therefore, it can be concluded that the utilization rate of copper tailings in China is far from that of foreign companies [12]. The low recovery and utilization of copper tailings have also led to serious environmental pollution during the tailing treatment process.

Due to the open-pit stacking method used to treat copper tailings in China, the current occupation area of mines in China has reached 65,000 square hectares, which brings a lot of negative impacts while occupying a large amount of land resources. It is estimated that copper tailing fertilizer will cause economic loss of more than 10 billion yuan [13]. In addition, due to the large number of copper tailing ponds in my country, the tailing dams are piled up upstream to store water. However, the tailing dam built therefrom may have a risk of dam failure due to the small particle size of the tailing particles and the poor cohesion between the particles. In recent years, the climate environment has changed greatly, and more than 10 dam-break accidents have occurred [14]. Extensive tailing treatment methods such as open-air stacking have also caused a lot of waste of resources. Due to the comprehensive utilization rate of copper tailings in China, the valuable metals in the tailings of the other party are wasted in large amounts. The increasingly serious problem of copper tailing treatment has also made the development and optimization of tailing treatment technology an important part of the development of a green and circular economy [15]. Figure 1 shows the current status of copper tailing treatment.

Figure 1: Current status of treatment of copper tailings.

The current methods of processing copper tailings in China mainly include three aspects: (1) as a secondary resource for recycling, (2) as a backfill for backfilling of mining goafs, and (3) according to the physical and chemical properties of copper tailings, the current recycling method for LSC tailings is mainly to use it as concrete. Concrete is the most widely used building material in the construction field. Copper tailing concrete has the possibility of realizing certain economic benefits [16]. However, the current research on copper tailings is mainly focused on the analysis of high-silicon copper tailings and their performance and characteristics when used as concrete materials. Therefore, the less studied LSC tailings are selected as the research objects in this study. The study of the PSD and performance of LSC tailings under the action of mechanical force provides a theoretical basis for the production and application of LSC tailing concrete.

2.2. Image Processing Technology Based on CNN. CNN is a feedforward neural network that includes convolutional calculations and has a deep structure. Its basic structure includes five structures: input layer, convolution layer, pooling layer, fully connected layer, and output layer. The structure of the neural network is shown in Figure 2. Firstly, the input layer reads the pixel matrix of the input image and outputs to a convolutional layer with multiple feature surfaces. There are multiple neurons for each feature surface, and the input of each neuron node is the convolution block of the previous network, and using the convolution block in the convolution layer can extract the depth information of the image and obtain higher-dimensional feature information [17]. The convolutional layer is to perform a convolution operation on the input original image to obtain the underlying features contained in the image. In the convolution process, the convolution kernel is used to extract the features of the input image. A convolution kernel can extract a kind of image feature, and each convolution kernel has a corresponding weight coefficient and offset [18].

The principle of parameter optimization of CNN is described as follows: it is assumed that each convolutional layer contains only one convolution kernel, and the convolution feature matrix is outputted after convolution calculation. The specific expression is given as follows:

$$C_i = f(W_i \otimes C_{i-1} + b_i). \tag{1}$$

In the above equation, W_i is the weight of the convolution kernel, $\otimes$ is the convolution calculation, b_i represents the node bias, $f()$ refers to the activation function, and C_{i-1} represents the convolution feature of the previous output. After the convolution operation, C_i enters the pooling layer for dimensionality reduction, and the characteristic obtained by sampling is S_i:

$$S_i = pooling(H_i). \tag{2}$$

In equation (2) above, $pooling()$ means pooling operation and H_i means the sliding window. After the image is feature extracted, the feature vector is input into the classifier for classification. The probability distribution of the completed input image for each category is shown as follows (of which n represents the category index):

$$l(W, b) = \frac{1}{N}\sum_{n=1}^{N}\left(Y(n) - Y^*(n)\right)^2. \tag{3}$$

In the above equation (3), $l(W, b)$ represents the probability distribution under the corresponding weight and bias, $Y()$ represents the output layer, $Y^*()$ refers to the expected output result, and N represents the total number of indexes. A loss function is constructed based on the output value and the actual value and added with a two-

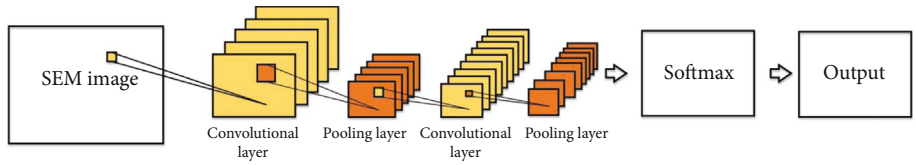

Figure 2: Structure of CNN.

norm term (L2-regularization) to prevent overfitting. The equation is expressed as follows (λ refers to the weight attenuation coefficient):

$$L(w,b) = \frac{1}{N}\sum_{n=1}^{N}\left(Y(n) - Y^{*}(n)\right)^{2} + \frac{\lambda}{2}W^{T}W. \quad (4)$$

$L(W,b)$ represents the probability distribution of the corresponding weight and offset after correction.

In the first-level convolution process, the convolution kernel scans the input image according to the step size and convolves the obtained data to obtain low-level features [19]. The nonlinear function is used for the obtained result to obtain the convolution graph of the first layer network. In the middle layer of the convolutional layer, the output result of the previous layer is trained and learned according to the weight parameters and offsets in the layer, and the image is convolved with different receptive fields of the same convolution kernel to reduce parameter settings to reduce the complexity of the network [20]. In the middle layer of the convolutional network, the high-level features of the image can be obtained through multiple feature extraction. The pooling layer performs dimensionality reduction operations on the high-level feature output by the convolutional layer. The neurons between the layers in the fully connected layer are fully connected, and the feature information obtained by the convolutional layer and the pooling layer is classified [21]. The output layer uses the Softmax function to classify features and output the results. After the probability distribution of each category is calculated, the category with the highest probability is the category of the test sample. Figure 3 is a model diagram of SEM image feature extraction based on CNN.

2.3. The Effects of Mechanical Force on the Particle Size and Activity of LSCT. The resource utilization methods of copper tailings include the recovery of valuable components and the preparation of building materials. Concrete is a kind of silicate product taking siliceous materials (sand, fly ash, silica-containing tailings, etc.) and calcareous materials (lime, cement, etc.) as raw materials and processing by batching, mixing, pouring, cutting, autoclaving, and curing, showing the advantages of firmness and fire resistance [22]. Therefore, using LSCT as a raw material for concrete can realize the resource utilization of tailing resources. However, the fineness of LSCT will affect the material properties of aerated concrete. Therefore, many studies have discussed the optimal fineness of LSCT to prepare aerated concrete. Relevant studies have shown that LSCT sand concrete shows good antisegregation ability, so using LSCT as a raw material can improve the elastic modulus and resistance to chloride ion permeability of concrete. In addition, the fixation of LSCT in concrete will also affect the preparation and performance of concrete and further reduce the heavy metal leaching rate of LSCT, which can well eliminate the impact of low-silicon copper tailings on the environment. In general, the formation of aerated concrete hydration products depends on the properties of the raw materials and the reaction conditions with the gel material; the interaction effect between the cementitious materials is related to the quality of the material gradation, but when the fineness of the material is good, it can slow down the speed of particle sedimentation and separation in the slurry and ensure the uniformity and foaming stability of the slurry [23]. In addition, LSCT, sand, cement, and other materials with appropriate fineness can maintain the slurry to undergo gassing at an appropriate thickening speed, and materials with appropriate fineness will also improve the hardening speed and early strength of aerated concrete ligands [24].

Relevant studies have shown that the fineness of LSCT will have a certain impact on the pouring stability of aerated concrete. The finer the particles of LSCT, the better the fluidity of the concrete during pouring, the larger the surface area of the LSCT particles participating in the reaction, and the stronger the activity [25]. However, it is easy to increase the consistency of the concrete slurry and cause insufficient gas generation, and the larger the particle size of LSCT, the worse the fluidity of the concrete and subsidence [26]. Therefore, it is very important to choose LSCT of appropriate fineness to prepare concrete. The fineness of copper tailings also affects important physical properties such as the absolute dry strength of aerated concrete. The finer the particle size of copper tailings, the less conducive to the formation of a good pore structure of concrete castings and the worse the cementing effect of concrete [27]. Therefore, studying the PSD of LSCT after the effect of mechanical force is of great significance to tailing recycling and production processing.

2.4. Particle Detection of LSCT Based on Image Processing Technology. LSCT particles have different particle forms and chemical compositions. The study of the PSD and physical and chemical properties of copper tailing particles plays an important role in the chemical properties, practical applications, and environmental impact of the particles. LSCT particles present different particle sizes under the action of mechanical force, which directly affects its properties when it is undertaken as concrete building materials [28, 29]. Among the analytical methods for studying LSCT particles, SEM can observe the microscopic morphology and particle size of tailing particles, and X-ray spectroscopy can obtain

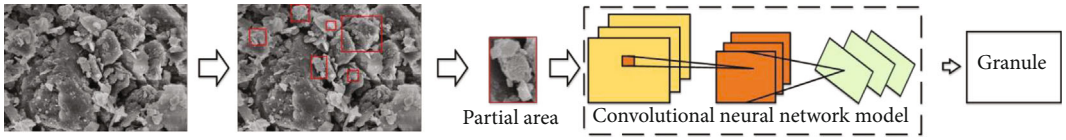

Figure 3: SEM image feature extraction model based on CNN.

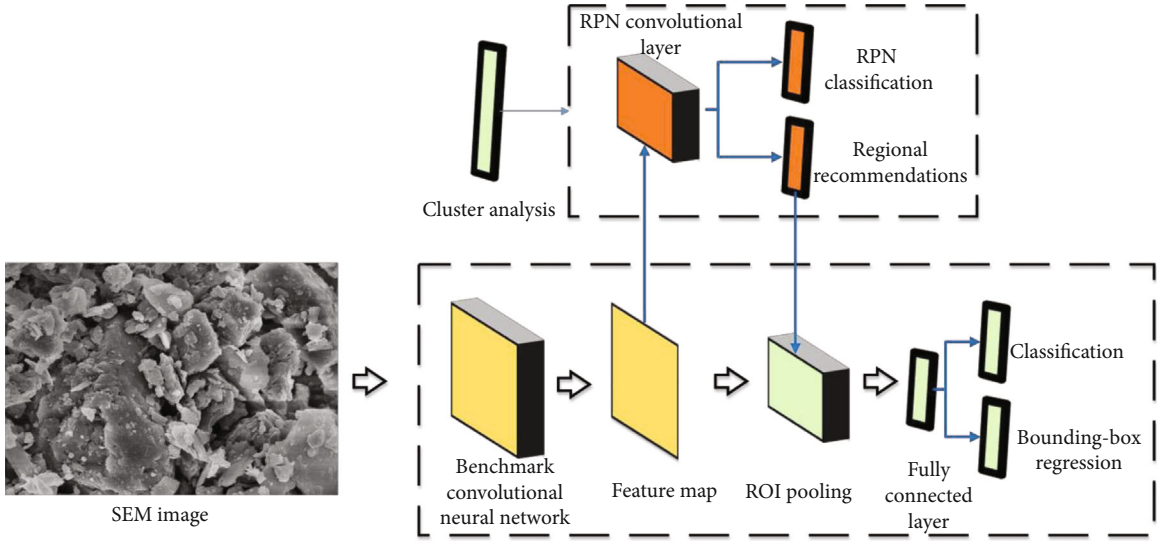

Figure 4: SEM image recognition model of LSCT based on Faster-R-CNN.

chemical information of tailing particles. As an important image recognition analysis technology, CNN shows a wide range of applications in image recognition. In this study, the particle morphology and PSD of LSCT are studied, and CNN and SEM images of LSCT are combined to identify and analyse different morphological features and particle sizes, aimed at providing reference for analysis of particle size and performance of LSCT under the action of mechanical force [30, 31].

Compared with traditional artificial networks, CNN shows the characteristics of local perception and weight sharing. Therefore, CNN can be used to establish a target detection algorithm with excellent performance. In the research, Faster-R-CNN with higher recognition accuracy is used as the image recognition model. Faster- R-CNN adds a region of interest pooling layer and a region proposal network (RPN) on the basis of CNN and proposed a loss function including the loss of classification of candidate regions and the loss of position regression [32]. Therefore, when the SEM image of LSCT particles is analysed, Faster-R-CNN can use the two-dimensional structure of the input SEM image [33]. During image processing, a large number of image parameters are reduced to a small number of parameters, without affecting the data characteristics of the SEM images of LSCT particles. Through the regular movement of the convolution kernel on the image, the features with the same structure in the image are captured to make a feature map. These features are the basis of image recognition. Figure 4 shows the SEM image recognition model of LSCT based on Faster-R-CNN.

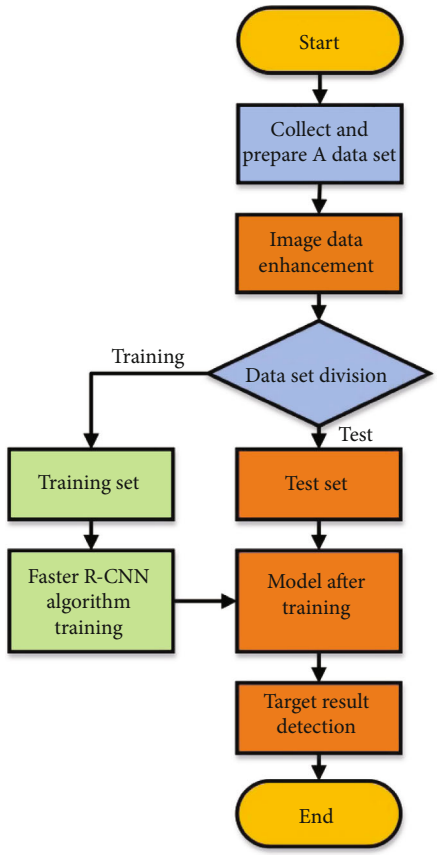

Figure 5: Design of SEM image recognition system of LSCT.

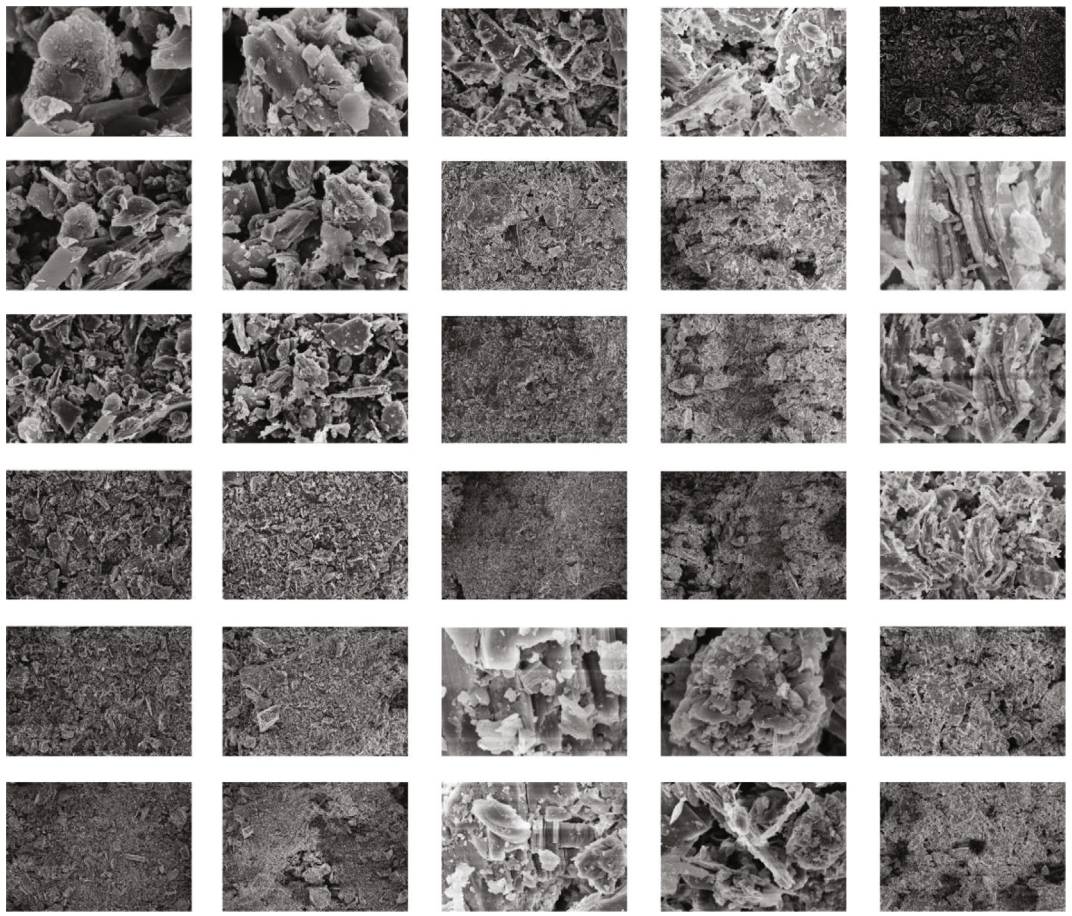

Figure 6: Data enhancement data set partial display.

Table 1: Setting of experimental information and network parameters.

Deep learning framework	TensorFlow	Learning rate	0.1
Training and testing data sets	ImageNet data set, LSC tailing SEM image data set	Batch size	256
System	Ubuntu 18.04	Number of iterations	60
CPU	i7-7700	Momentum	0.9
GPU	NVIDIA GTX 1080	Loss function	Exponential loss
Hard drive capacity	16 GB + 1 TB	Number of hidden layer units	100

The SEM images of copper tailing particles are classified and identified based on CNN, the corresponding algorithm framework is established, and the model is trained [34]. The commonly used benchmark CNNs in Faster-R-CNN include VGGNet, ResNet, and DenseNet. In this study, DenseNet, which is resistant to overfitting, is undertaken as the convolutional layer of Faster-R-CNN to extract image features and is compared with VGG16 (VGGNetyou 16-layer network structure), ResNet50 (50-layer network structure), and ResNet101 (101-layer network structure) to analyse the performance. Figure 5 shows the recognition flow of the designed SEM image of LSCT.

2.5. Raw Material Preparation and Test Methods. The WAM-5L horizontal ball mill (mill speed is 140 r/min, ball grading is large ball : medium ball : small ball = 2 : 5 : 3, ball-to-battery ratio is 3 : 1) is adopted to grind the LSCT. Grinding time is 0 min, 30 min, 60 min, 90 min, 120 min, 150 min, and 180 min, and a total of 7 groups of low-silicon copper tailing samples take 1 g each. The morphology of each group of LSCT samples is observed under SEM to analyse the appearance and surface morphology of LSCT particles. A laser particle size analyser is used for particle size testing and analysis; the crystal structure and chemical composition are analysed by XRD. Surface functional groups, molecular structure, and valence bond interactions are analysed by FTIR [35].

To observe the microstructure of the LSC tailings by SEM images, the PSD of the LSC tailings is indirectly understood, and then, the performance of the LSC tailings is understood. In the study, computer image processing technology is used to quickly count the PSD of LSC tailings after

mechanical force and provide an effective analysis method for the comprehensive utilization of copper tailings. Since the PSD is monitored in the SEM image of LSC tailings in this study, there is no relevant public data set. Therefore, in the research process, SEM images of LSC tailings are obtained through experiments, and the collected LSC tailing SEM images of different mechanical force grinding times are made into a data set according to the PASCAL VOC image data set standard. According to the scale of the SEM image, the data set is divided into 6 categories: 1 μm, 2 μm, 5 μm, 20 μm, 50 μm, and 100 μm. Figure 6 shows part of the data augmentation data set. In order to prevent the occurrence of model overfitting and failure to converge, the images in the data set are enhanced. Specific operations include rotation, noise reduction, adjustment of saturation, contrast, brightness, and sharpness. Table 1 shows the relevant settings of the experimental parameters.

3. Characterization Test and Model Performance Comparison

3.1. CNN Training. To better use the SEM image recognition network to identify the particle distribution of LSC tailings, in the image recognition network training process, the number of batch samples from 1 to 100 is tested with iterations of 5, 10, 20, and 30, respectively, to determine the number of batch samples of model samples. The results are shown in Figure 7.

As shown in Figure 7, the number of batch samples is negatively correlated with the LSC tailing SEM image recognition accuracy. As the number of samples in the model batch increases, accuracy shows a downward trend, but when the number of iterations is 50-60, accuracy drops significantly. Therefore, the number of batch samples used in the study is 50 to balance the relationship between the number of batch samples and the number of iterations. It can be obtained from the relationship between the number of iterations and accuracy that when the number of iterations is less than 10, the two show a positive correlation, but after the number of iterations exceeds 10, the accuracy does not change. Therefore, the number of iterations in the study is set to 60 to ensure the accuracy and computational performance of the model.

3.2. The Effect of Mechanical Force Action Time on the PSD of LSC Tailings. The particle size and distribution of LSCT will change under the action of mechanical force. To verify the crystal structure, chemical composition, and particle size distribution of LSCT under the action of mechanical force, the LSCT are characterized and tested by XRD, FTIR, and laser particle size analyser. The XRD and infrared test results are shown in Figures 8(a) and 8(b), and the test results of the laser particle size analyser are shown in Figures 9(a) and 9(b).

Figure 8(a) illustrates that the main components of LSCT include carbonates, silicates, and silicates such as quartz, calcite, illite, and andradite, and the content of quartz is the largest. The infrared characterization results in Figure 8(b) show that the mechanical force effect does not

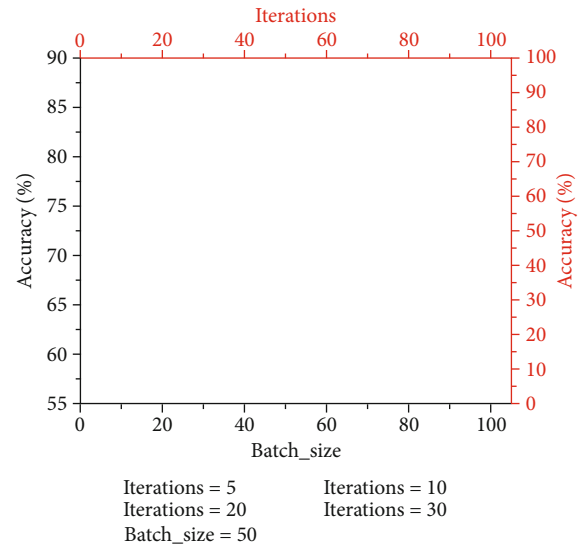

FIGURE 7: The impact of different batch samples and iteration times on the recognition effect.

cause the chemical composition of the LSCT to change. As given in Figures 9(a) and 9(b), the mechanical force greatly reduces the particle size of LSCT and can effectively improve the particle size distribution of LSCT. Without mechanical force, the particle size of LSCT is mainly concentrated 100~1000 μm. After 30 minutes of mechanical force, the PSD of LSCT is mainly concentrated 1~100 μm, of which the PSD of LSCT of about 1.4 μm and 10 μm is the most. With the increase of mechanical force action time, the amount of PSD of LSCT of about 10 μm decreases, the PSD of LSCT of about 1.4 μm increases, and the trend of change gradually decreases in the later period. When the grinding time reaches 150 minutes, the particle size of the LSCT reaches the minimum, and the particle size starts to increase after grinding for 180 minutes. The reason for this phenomenon may be that the particle size of the LSCT becomes smaller, the specific surface area increases, and the surface activity increases, which makes the LSCT particles agglomerate, increasing the test results.

3.3. Model Performance Test. In the study, the SEM image detection model based on Faster R-CNN and DenseNet was compared with other models. Under the training of the ImageNet data set, the prepared SEM image data set of LSC tailings is tested, and the detection results of each different target are obtained. The average accuracy is used as the evaluation standard. The test comparison results are shown in Figure 10.

Figure 10(a) illustrates that the average recognition accuracy of the design model on the SEM image of LSC tailing particles is 86.97%, and the average recognition accuracy of the voids is 89.03%. Due to the recognition results of SEM images of LSC tailings by other models, the designed network model has relatively good performance and can extract more features of the target. As illustrated in Figure 10(b), the DenseNet used a small amount of parameters, but it takes a long time to detect the target, which is

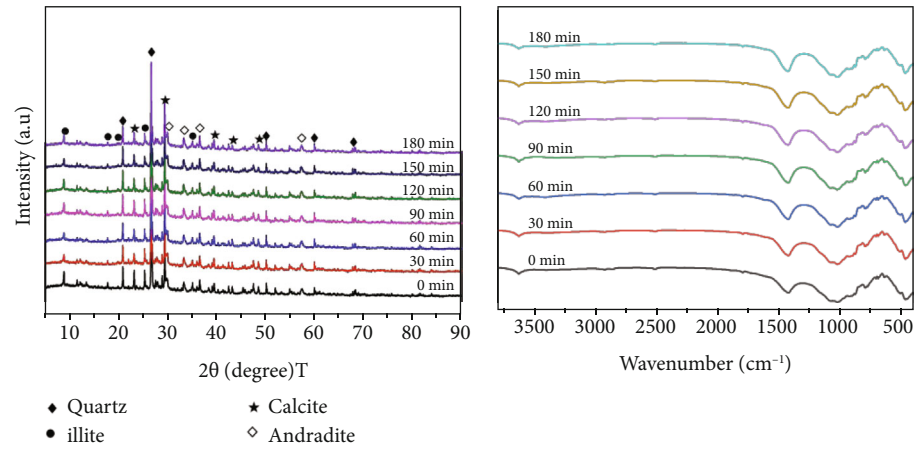

(a) XRD test results (b) Infrared test results

Figure 8: XRD and infrared test results of LSC tailings.

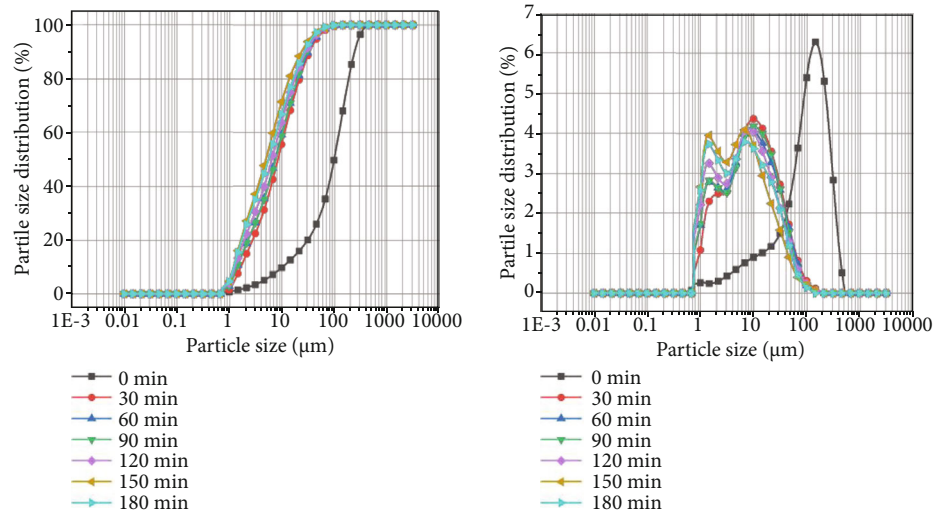

(a) Cumulative distribution of LSC tailing particle size (b) PSD of LSC tailings

Figure 9: Laser particle size analyser test results of LSC tailings.

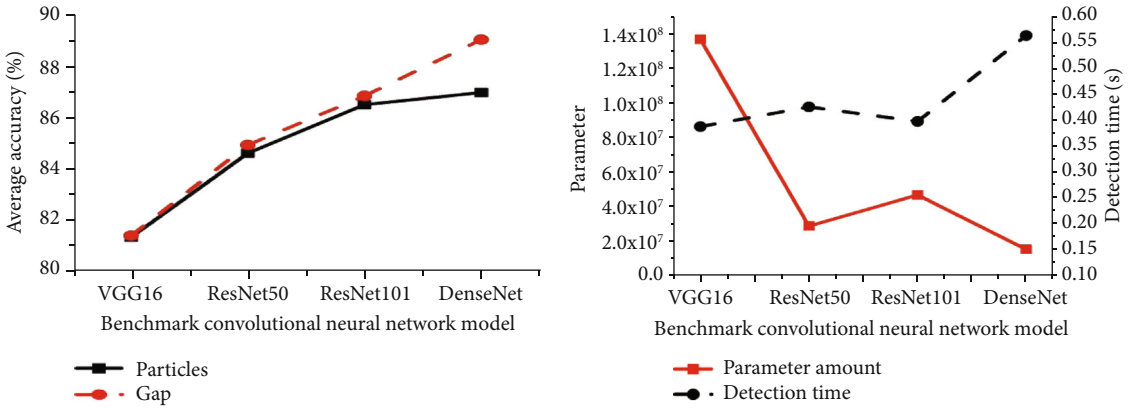

(a) Comparison on average accuracy (b) Comparison of model parameters and detection time

Figure 10: Comparison test of model performance.

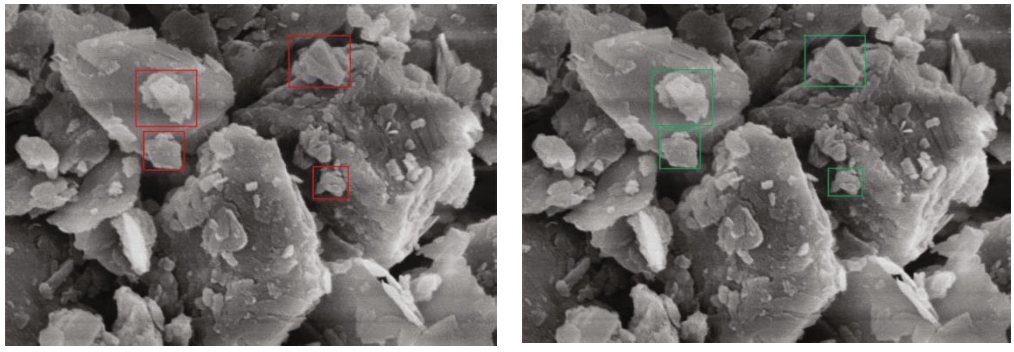

(a) VGG16 (b) ResNet50

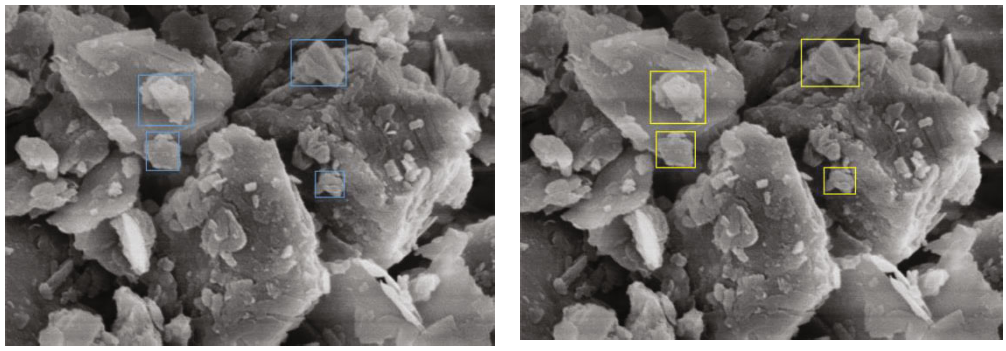

(c) ResNet101 (d) DenseNet

Figure 11: Feature extraction effect of Faster-R-CNN on LSC tailing SEM image.

slower than the target recognition of other models. The reason may be that DenseNet has a 169-layer network structure, so although the number of parameters of the model is small, the detection time of the target is longer. In addition, the feature map of DenseNet is larger than that of other models, which leads to an increase in the amount of calculation for convolution calculations and a larger memory usage, which in turn leads to more time consumption.

3.4. Target Detection Effect. The Faster R-CNN algorithm is used to extract the features of the prepared LSC tailing SEM image data set, and the collected data is abstracted by layer-by-layer stacking. The recognition effect of the SEM image of LSC tailings using different benchmark CNN models is shown in Figure 11.

Figure 11 reveals that the Faster-R-CNN models using VGG16, ResNet50, ResNet101, and DenseNet have relatively close detection results for LSC tailing particles, so these models can be used to effectively detect copper tailing particles. The detection result of Faster-R-CNN based on DenseNet is more accurate, and it has a good performance in the extraction of LSC tailing SEM image data. By stacking layer by layer, the extracted data is combined into abstract features, so it has high accuracy in image recognition.

3.5. The Effect of Mechanical Force on the Activity of LSC Tailings. Figure 12 shows the relationship between compressive strength ratio (activity index) and grinding time of the prepared mortar test block and the reference group (mixing amount 0) prepared with LSCT (30% content) when the grinding time is 0 min, 30 min, 60 min, 90 min, 120 min, 150 min, and 180 min.

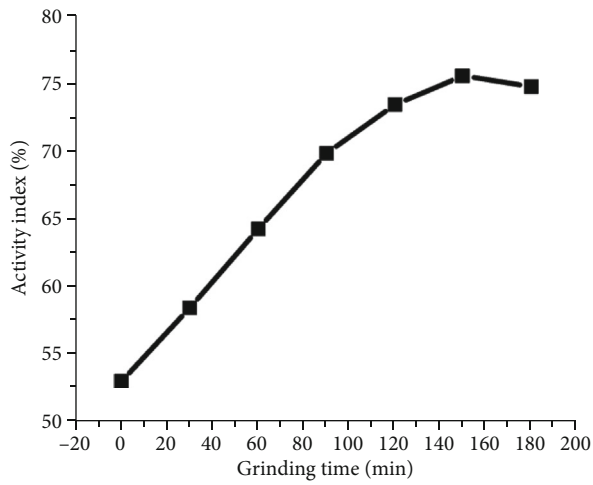

Figure 12: The relationship between LSC tailing grinding time and activity index.

As given in Figure 12, the activity index of LSCT in an alkaline environment is 52.959% when the mechanical force is not applied, which does not meet the minimum activity index requirement for admixtures in concrete engineering. Within 30~120 minutes, with the increase of action time of mechanical force, the activity index of LSCT in alkaline environment is constantly improved, reaching 73.422% at the 120th minute. The reason is that during the grinding process

of LSCT, the particles appear to crack, the crystal lattice is distorted, and the crystallinity drops or even reaches an amorphous state, which leads to the activation of the LSCT in an alkaline environment. After 120~180 minutes, the increasing trend of activity decreases and begins to decrease at the 180th minute; it reaches the maximum at the 150th minute, the activity index is 75.545%, and it drops to 74.735% at 180 minutes. The reason for the decline may be that the LSCT have agglomerated, which leads to an increase in particle size and affects activity.

4. Conclusion

To understand the performance status of LSCT under the action of mechanical force, the LSCT under different grinding times are explored in this study. Based on analysis of the current utilization status of copper tailings in China and the influence of its fineness and activity on the preparation and performance of aerated concrete, it is proposed to combine the image processing technology to analyse the scanning electron microscopy images of the LSCT under the action of mechanical force and to train and adjust the parameters of the CNN-based image recognition model to improve the image recognition accuracy of the model. Finally, the experimental process is designed, the collected LSCT SEM images are used as a data set, and the model is trained through the training set. In addition, the image recognition test is performed on the produced data set. The results show that when the number of CNN iterations is 10, the accuracy of the model and recognition can be guaranteed. The PSD of LSCT under the action of mechanical force is mainly concentrated in 1.4 μm~10 μm; the particle size of the LSCT reaches the minimum when grinding for 150 minutes, and the activity index also reaches the maximum. The average accuracy of SEM image detection of the model is 86.97%, and the designed model has better recognition accuracy compared with other models. However, there are still some shortcomings in this study. The segmentation of the image will cause the recognition accuracy of the model to decrease, so the model needs to be further optimized in the follow-up.

Data Availability

The data used to support the findings of this study are included within the article.

Conflicts of Interest

The authors declare that they have no conflicts of interest.

Acknowledgments

This achievement was financially supported by the National Key R&D Project of China (2019YFC1904103).

References

[1] H. Jin, L. Lin, X. Meng et al., "A novel lanthanum-modified copper tailings adsorbent for phosphate removal from water," *Chemosphere*, vol. 281, article 130779, 2021.

[2] L. S. Wong-Pinto, A. Mercado, G. Chong, P. Salazar, and J. I. Ordóñez, "Biosynthesis of copper nanoparticles from copper tailings ore - an approach to the 'bionanomining'," *Journal of Cleaner Production*, vol. 315, article 128107, 2021.

[3] R. Dandautiya and A. P. Singh, "Utilization potential of fly ash and copper tailings in concrete as partial replacement of cement along with life cycle assessment," *Waste Management*, vol. 99, pp. 90–101, 2019.

[4] L. Tao, L. Wang, K. Yang, X. Wang, L. Chen, and P. Ning, "Leaching of iron from copper tailings by sulfuric acid: behavior, kinetics and mechanism," *RSC Advances*, vol. 11, no. 10, pp. 5741–5752, 2021.

[5] S. Li, Z. Guo, J. Pan, D. Zhu, T. Dong, and S. Lu, "Stepwise utilization process to recover valuable components from copper slag," *Minerals*, vol. 11, no. 2, p. 211, 2021.

[6] X. Li, N. Zhang, J. Yuan et al., "Preparation and microstructural characterization of a novel 3D printable building material composed of copper tailings and iron tailings," *Construction and Building Materials*, vol. 249, article 118779, 2020.

[7] X. Lv, W. Shen, L. Wang, Y. Dong, J. Zhang, and Z. Xie, "A comparative study on the practical utilization of iron tailings as a complete replacement of normal aggregates in dam concrete with different gradation," *Journal of Cleaner Production*, vol. 211, pp. 704–715, 2019.

[8] D. M. Xu, C. L. Zhan, H. X. Liu, and H. Z. Lin, "A critical review on environmental implications, recycling strategies, and ecological remediation for mine tailings," *Environmental Science and Pollution Research*, vol. 26, no. 35, pp. 35657–35669, 2019.

[9] M. Fisonga, F. Wang, and V. Mutambo, "Sustainable utilization of copper tailings and tyre-derived aggregates in highway concrete traffic barriers," *Construction and Building Materials*, vol. 216, pp. 29–39, 2019.

[10] Z. Chen, X. Liu, J. Yang, E. Little, and Y. Zhou, "Deep learning-based method for SEM image segmentation in mineral characterization, an example from Duvernay Shale samples in Western Canada Sedimentary Basin," *Computers & Geosciences*, vol. 138, article 104450, 2020.

[11] Q. Zeng, S. Wang, L. Hu et al., "Oxalic acid modified copper tailings as an efficient adsorbent with super high capacities for the removal of Pb^{2+}," *Chemosphere*, vol. 263, article 127833, 2021.

[12] S. Liu, L. Wang, Q. Li, and J. Song, "Hydration properties of Portland cement-copper tailing powder composite binder," *Construction and Building Materials*, vol. 251, article 118882, 2020.

[13] S. Jian, W. Gao, Y. Lv et al., "Potential utilization of copper tailings in the preparation of low heat cement clinker," *Construction and Building Materials*, vol. 252, article 119130, 2020.

[14] A. Zhang, Z. Zou, Y. Liu et al., "Automated detection of circulating tumor cells using faster region convolution neural network," *Journal of Medical Imaging and Health Informatics*, vol. 9, no. 1, pp. 167–174, 2019.

[15] A. B. Botelho Junior, D. B. Dreisinger, and D. C. R. Espinosa, "A review of nickel, copper, and cobalt recovery by chelating ion exchange resins from mining processes and mining tailings," *Mining, Metallurgy & Exploration*, vol. 36, no. 1, pp. 199–213, 2019.

[16] T. Jia, Y. Wang, and B. Chai, "Bacterial community characteristics and enzyme activities in Bothriochloa ischaemum litter

over progressive phytoremediation years in a copper tailings dam," *Frontiers in Microbiology*, vol. 11, p. 3344, 2020.

[17] J. Jiang, Q. Cai, B. Ma et al., "Effect of ZSM-5 waste dosage on the properties of autoclaved aerated concrete," *Construction and Building Materials*, vol. 278, article 122114, 2021.

[18] X. Zhang, K. Wei, X. Kang, and J. Li, "Hybrid nonlinear convolution filters for image recognition," *Applied Intelligence*, vol. 51, no. 2, pp. 980–990, 2021.

[19] F. Li, G. Chen, Y. Zhang, Y. Hao, and Z. Si, "Fundamental properties and thermal transferability of masonry built by autoclaved aerated concrete self-insulation blocks," *Materials*, vol. 13, no. 7, p. 1680, 2020.

[20] X. Liu, H. Wang, H. Jing, A. Shao, and L. Wang, "Research on intelligent identification of rock types based on faster R-CNN method," *Ieee Access*, vol. 8, pp. 21804–21812, 2020.

[21] R. Agbozo and W. Jin, "Quantitative metallographic analysis of GCr15 microstructure using mask R-CNN," *Journal of the Korean Society for Precision Engineering*, vol. 37, no. 5, pp. 361–369, 2020.

[22] L. Cai, X. Li, W. Liu, B. Ma, and Y. Lv, "The slurry and physical-mechanical performance of autoclaved aerated concrete with high content solid wastes: effect of grinding process," *Construction and Building Materials*, vol. 218, pp. 28–39, 2019.

[23] G. Pachideh and M. Gholhaki, "Effect of pozzolanic materials on mechanical properties and water absorption of autoclaved aerated concrete," *Journal of Building Engineering*, vol. 26, article 100856, 2019.

[24] J. Jiang, B. Ma, Q. Cai et al., "Utilization of ZSM-5 waste for the preparation of autoclaved aerated concrete (AAC): mechanical properties and reaction products," *Construction and Building Materials*, vol. 297, article 123821, 2021.

[25] X. Rao, F. Lin, Z. Chen, and J. Zhao, "Distracted driving recognition method based on deep convolutional neural network," *Journal of Ambient Intelligence and Humanized Computing*, vol. 12, no. 1, pp. 193–200, 2021.

[26] Q. Li and G. Chen, "Recognition of industrial machine parts based on transfer learning with convolutional neural network," *PLoS One*, vol. 16, no. 1, article e0245735, 2021.

[27] Y. Peng, Y. Liu, B. Zhan, and G. Xu, "Preparation of autoclaved aerated concrete by using graphite tailings as an alternative silica source," *Construction and Building Materials*, vol. 267, article 121792, 2021.

[28] M. Shen, G. Li, D. Wu et al., "Multi defect detection and analysis of electron microscopy images with deep learning," *Computational Materials Science*, vol. 199, article 110576, 2021.

[29] H. Zhang, G. Wang, Y. Li, and H. Wang, "Faster R-CNN, fourth-order partial differential equation and global-local active contour model (FPDE-GLACM) for plaque segmentation in IV-OCT image," *Signal, Image and Video Processing*, vol. 14, no. 3, pp. 509–517, 2020.

[30] W. Sun, H. Gao, S. Tan, Z. Wang, and L. Duan, "Wear detection of WC-Cu based impregnated diamond bit matrix based on SEM image and deep learning," *International Journal of Refractory Metals and Hard Materials*, vol. 98, article 105530, 2021.

[31] K. Shaga Devan, P. Walther, J. von Einem, T. Ropinski, H. A Kestler, and C. Read, "Improved automatic detection of herpesvirus secondary envelopment stages in electron microscopy by augmenting training data with synthetic labelled images generated by a generative adversarial network," *Cellular Microbiology*, vol. 23, no. 2, article e13280, 2021.

[32] W. Yu, Y. Xue, R. Knoops et al., "Automated diatom searching in the digital scanning electron microscopy images of drowning cases using the deep neural networks," *International Journal of Legal Medicine*, vol. 135, no. 2, pp. 497–508, 2021.

[33] Z. Yue, F. Gao, Q. Xiong et al., "A novel semi-supervised convolutional neural network method for synthetic aperture radar image recognition," *Cognitive Computation*, vol. 13, no. 4, pp. 795–806, 2021.

[34] W. L. Mao, W. C. Chen, C. T. Wang, and Y. H. Lin, "Recycling waste classification using optimized convolutional neural network," *Resources, Conservation and Recycling*, vol. 164, article 105132, 2021.

[35] Y. An, J. Guo, Q. Ye, C. Childs, J. Walsh, and R. Dong, "Deep convolutional neural network for automatic fault recognition from 3D seismic datasets," *Computers & Geosciences*, vol. 153, article 104776, 2021.